Acta Crystallographica Section B
Structural Science
ISSN 0108-7681

Structure of $C_nC_{n+2}C_n$-type (n = even) β'-triacylglycerols

Arjen Van Langevelde,[a]* Kees Van Malssen,[a] René Driessen,[a] Kees Goubitz,[a] Frank Hollander,[b] René Peschar,[a] Peter Zwart[a] and Henk Schenk[a]

[a]Laboratory for Crystallography, Institute for Molecular Chemistry (IMC), Universiteit van Amsterdam, Nieuwe Achtergracht 166, 1018 WV Amsterdam, The Netherlands, and [b]RIM Department of Solid State Chemistry, University of Nijmegen, Toernooiveld, 6525 ED Nijmegen, The Netherlands

Correspondence e-mail: arjen@crys.chem.uva.nl

Received 3 July 2000
Accepted 17 July 2000

The crystal structures of the β' phase of CLC (1,3-didecanoyl-2-dodecanoylglycerol) and MPM (1,3-ditetradecanoyl-2-hexadecanoylglycerol) have been determined from single-crystal X-ray diffraction and high-resolution X-ray powder diffraction data, respectively. Both these crystals are orthorhombic with space group $Iba2$ and $Z = 8$. The unit-cell parameters of β'-CLC are $a = 57.368$ (6), $b = 22.783$ (2) and $c = 5.6945$ (6) Å and the final R value is 0.175. The unit-cell parameters of β'-MPM are $a = 76.21$ (4), $b = 22.63$ (1) and $c = 5.673$ (2) Å and the final R_p value is 0.057. Both the β'-CLC and β'-MPM molecules are crystallized in a chair conformation, having a bend at the glycerol moiety. The zigzag planes of the acyl chains are orthogonally packed, as is typical for a β' phase. Furthermore, unit-cell parameters of some other members of the $C_nC_{n+2}C_n$-type triacylglycerol series have been refined on their high-resolution X-ray powder diffraction pattern. Finally, the crystal structures are compared with the currently known structures and models of triacylglycerols.

1. Introduction

Triacylglycerols (TAGs) are esterifications of three long-chain fatty acids with glycerol. Many different types of TAGs exist because the three fatty acids can all differ in chain length and degree of saturation. Natural oils and fats are complex mixtures of these various TAG types and are applied in a wide range of consumer products, such as foods, cosmetics and medicine. Typical physical properties of TAG mixtures such as solidification, melting and polymorphic behaviour give each product its own characteristics (Sato, 1996). For example, the spreadability of butter and lipstick, hardness of chocolate, quality of ointments, and the consistency of whipped cream are all determined by the polymorphic phase of the fat component. Likewise, temperature-dependent polymorphic phase transitions are held responsible for product degradation, *e.g.* fat-bloom formation at the chocolate surface. To understand the complex crystallization processes and totally control the manufacturing processes, crystal-structure information of various TAG polymorphs is indispensable.

TAGs and their mixtures crystallize in the different polymorphic phases α, β and/or β' and sometimes several different β' and/or β polymorphs exist (Simpson & Hagemann, 1982; Arishima & Sato, 1989). Phase transformations of most TAGs ($\alpha \rightarrow \beta'$, $\alpha \rightarrow \beta' \rightarrow \beta$ or $\alpha \rightarrow \beta$) are monotropic, resulting in only one stable phase, β' or β, depending on the TAG type (Hagemann, 1988). For $C_nC_nC_n$-type (n = even) TAGs the most stable phase is β, whereas for $C_nC_{n+2}C_n$ and $C_nC_{n+4}C_{n+2}$-type (n = even) TAG series the β'-phase is the

most stable (De Jong, 1980). Furthermore, the relative phase stability is determined by the degree of saturation.

X-ray powder diffraction (XRPD) is commonly used to distinguish between the various polymorphs, since each polymorph has its own characteristic powder diffraction pattern originating from the typical packing of the long hydrocarbon chains. However, for complete structural information single crystals are essential and these are difficult to grow. Therefore, only crystal structures of the β polymorph of 1,2,3-tridecanoylglycerol (CCC), 1,2,3-tridodecanoylglycerol (LLL), 1,2,3-trihexadecanoylglycerol (PPP) and 2–11-bromoundecanoyl-1,3-didecanoylglycerol ($CL^{Br}C$) are known (Doyne & Gordon, 1968; Gibon *et al.*, 1984; Jensen & Mabis, 1963, 1966; Larsson, 1965*a*; Van Langevelde, Van Malssen, Hollander *et al.*, 1999). They crystallize in space group $P\bar{1}$, having an asymmetric 'tuning-fork' conformation, characterized by the two outer acyl chains (I) and (III) pointing in one direction and the middle one (II) in the opposite direction (Fig. 1). The molecules are packed like stacked chairs and the zigzag planes of all hydrocarbon chains are parallel, which is typical for a β polymorph (Abrahamsson *et al.*, 1978). Recently, Van Langevelde, Van Malssen, Hollander *et al.* (1999) showed the structural correspondence of this β-$C_nC_nC_n$-type (n = even) TAG series. Even the crystal structure of $CL^{Br}C$, a heavy-atom analogue of the $C_nC_{n+2}C_n$-type (n = even) and therefore expected to be β'-stable, was crystallized in the β polymorph (De Jong & Van Soest, 1978).

So far, efforts made to determine the crystal structure of TAGs in the β' phase were not successful. The growing of reasonable single crystals and the typical diffraction character were major problems in most trials. Nevertheless, unit-cell parameters and space groups of β'-LLL, β'-PSP (β'-1,3-dihexadecanoyl-2-octadecanoylglycerol), β'-$C_{11}C_{11}C_{11}$(β'-1,2,3-triundecanoylglycerol) and β'-LML (β'-1,3-didodecanoyl-2-tetradecanoylglycerol) were determined from single crystals (Birker *et al.*, 1991; Hernqvist, 1988; Hernqvist & Larsson, 1982; Larsson, 1965*b*). On the basis of packing arguments acyl chains were suggested to be tilted with respect to the methyl end-group plane. The direction of this tilt was expected to alternate between successive chain layers. Recently, from powder diffraction data, cell parameters and the space group *Iba*2 were determined for the β' polymorph of the $C_nC_{n+2}C_n$-type (n = even) TAG series (Van Langevelde, Van Malssen, Sonneveld *et al.*, 1999). Based on this information it was argued that straight TAG molecules without chain tilts may result in a plausible model for the structure of the β' polymorph. However, all these β' models are packing models only and provide no definite structural detail.

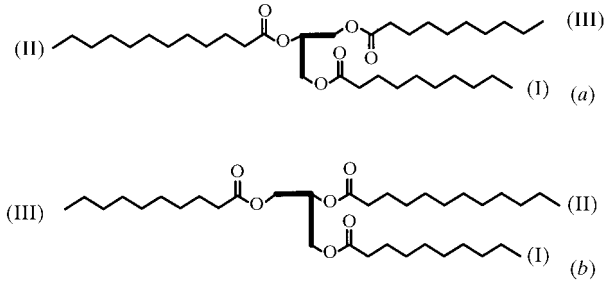

Figure 1
(*a*) Schematic representation of a tuning-fork conformation. (*b*) Schematic representation of a chair conformation. In both (*a*) and (*b*) the orientation of carbonyl and the zigzag planes are randomly chosen.

Until now, the only crystal structure model of a β' polymorph at the atomic level was published by Van de Streek *et al.* (1999). They constructed a model for the β' polymorph of CLC originating from the crystal structures of n-$C_{28}H_{58}$ (octacosane; Boistelle *et al.*, 1976) and PP2 (1,2-dihexadecanoyl-3-acetyl-*sn*-glycerol; Goto *et al.*, 1992). Since the structure of n-$C_{28}H_{58}$ has the desired chain packing and the structure of PP2 the desired chair conformation, parts of both structures were combined in one model. The calculated powder diagram of this model is in good agreement with the experimental one.

Here we report the first experimental crystal structure of a TAG in the β' polymorph. The structure of β'-CLC (β'-1,3-didecanoyl-2-dodecanoylglycerol), a $C_nC_{n+2}C_n$-type (n = even) TAG, has been determined from single-crystal X-ray diffraction data. Furthermore, the crystal structure of β'-MPM (β'-1,3-ditetradecanoyl-2-hexadecanoylglycerol), another series member, has been determined from high-resolution XRPD data. Finally, these structures are compared with existing β' models.

2. Materials and methods

2.1. Samples, sample preparation and data collection

A series of $C_nC_{n+2}C_n$-type (n = even) TAGs (CLC, LML, MPM and PSP) was obtained from Unilever Research Laboratory (Vlaardingen, The Netherlands), where the TAGs had been synthesized and subsequently purified with the Midget Rapid Zone Refiner X-521 (Enraf–Nonius, Delft, The Netherlands).

Many small crystals of the purified CLC were obtained from the melt using a cold finger. These small crystals were used as seeds mounted on a metal wire to induce crystallization from molten CLC, which was kept a few degrees below its melting point. Among the many crystals obtained *via* this method only a few turned out to be good enough for use in a single-crystal diffraction experiment.

The X-ray diffraction data of a CLC single crystal (0.8 × 0.04 × 0.005 mm) were collected at beamline ID11 (ESRF, Grenoble, France; Kvick & Wulff, 1992) using a monochromatic beam with a fixed wavelength of 0.5061 Å. Images having a maximal d-spacing resolution of 0.936 Å were made at room temperature using a Siemens CCD camera with an exposure time of 3 s. The crystal was rotated over a φ range of 0–360° with a stepsize of 0.3° at ω of 160 and 340°. The spots, which were collected from the images, were indexed using the program *SMART* (Bruker AXS Inc., 1998) resulting in an orthorhombic cell with axis lengths a = 57.368 (6), b = 22.783 (2) and c = 5.6945 (6) Å, and space group *Iba*2. With 8

molecules in the unit cell having a volume of 7443 (1) Å^3 this results in a calculated density of 1.04 Mg m^{-3}. The data were integrated using the program *SAINT* (Bruker AXS Inc., 1996), resulting in a total of 5706 reflections within the range $-52 \leq h \leq 51$, $-20 \leq k \leq 20$ and $-6 \leq l \leq 5$, corresponding with a $(\sin\theta)/\lambda$ range of 0.0236–0.5344 Å^{-1}. Merging equivalent and Friedel reflections yielded 1642 unique reflections, which is a completeness of 66%. Of these, 824 reflections were above the significance level of $3.5\sigma(F)$ and were treated as observed. The intensity of the strongest reflections could not be determined accurately since they exceeded the dynamic range of the detector.

XRPD patterns of LML, MPM and PSP were obtained with the high-resolution powder diffractometer at beamline BM16 (ESRF, Grenoble, France; Fitch, 1996) using a monochromatic beam with a fixed wavelength of 0.650515 (1) Å for MPM and 0.445348 (1) Å for LML, MPM and PSP. XRPD data were collected from capillaries with a diameter of 1.5 mm filled with powdered TAG, which were rotating during exposure. Continuous scans were made of an MPM sample at room temperature from 0.0 to 37.0° 2θ with 0.5° 2θ min^{-1} and a sampling time of 50 ms. After data collection this scan was binned at 0.003° 2θ. LML, MPM and PSP samples were scanned at a temperature of 250 K from 0.0 to 52.0° 2θ with 0.5° 2θ min^{-1} and a sampling time of 50 ms. After data collection these scans were binned at 0.005° 2θ.

2.2. Structure determination of β'-CLC from single-crystal data

Attempts to solve the crystal structure of CLC with standard structure determination packages were unsuccessful due to the small number of available reflections at atomic resolution and the unusual ratio between the cell axes. Finally, employing all 1642 unique reflections, a partial trial structure was generated using the macromolecular structure determination program *Shake-and-Bake*, version 1.5 (Miller *et al.*, 1994) and manual interference. This incomplete model (25 atoms) was refined using the unrestrained maximum-likelihood method *REFMAC* (Murshudov *et al.*, 1997), as available in the *CCP*4 package (Number 4 Collaborative Computational project, 1994). The structure was manually updated using the visualization program *O* (Jones *et al.*, 1991) employing $2mF_o - DF_{\rm calc}$ electron density maps. Using this procedure the structure was completed after three cycles. The structure was further refined using *Xtal* (Hall *et al.*, 1995) with an isotropic block-diagonal least-squares refinement on $|F|$ employing 824 observed reflections. The refinement converged to an R value of 0.175 and a maximum Δ/σ of 0.24. Soft bond and angle restraints on all non-H atoms were used, resulting in a total of 167 variables. H atoms with $U = 0.1$ Å^2 were calculated at 1.0 Å of their carrier atom and kept fixed during refinement. A final ΔF synthesis revealed a residual electron density between −1.2 and 1.1 e Å^{-3} in the vicinity of the glycerol moiety.

2.3. Structure determination of other series members from powder data

Cell parameters of β'-LML, β'-MPM and β'-PSP, as determined by Van Langevelde, Van Malssen, Sonneveld *et al.* (1999), were refined on their synchrotron diffraction patterns using the program *UnitCell* (Holland & Redfern, 1997).

To obtain accurate reflection intensities a full-pattern decomposition (FPD) procedure was started for the orthorhombic crystallized β'-MPM. The high-resolution synchrotron powder diffraction pattern was fitted employing a split-type pseudo-Voigt peak-profile function (Toraya, 1986) and decomposed using the program *MRIA* (Zlokazov & Chernyshev, 1992). Since the molecular structure of the $C_nC_{n+2}C_n$-type (n = even) TAGs differ by the length of the acyl chains only, and since the melting points of their β' polymorphs lie on a smooth curve (Birker *et al.*, 1991), this series can be considered as homologous. Therefore, a structural model for β'-MPM has been made using the program *Cerius*^{2} (Molecular Simulations Inc., 1995), starting from the crystal structure of β'-CLC. The terminating H atoms of all acyl chains were replaced by a $-(CH_2-CH_2)_2-H$ fragment. To position this possible model in the asymmetric unit of the refined unit cell with space group *Iba*2, a grid-search procedure (Chernyshev & Schenk, 1998) was applied using the reflection intensities obtained from the FPD procedure. The obtained translational and rotational parameters were refined followed by a bond-restrained Rietveld refinement (*RR*). During refinement soft restraints were applied to the atomic distances (σ is ∼1% of the ideal bond lengths). Under these restrictions the coordinates of all atoms (O, C and H) as well as isotropic atomic displacement parameters ($U_{\rm iso}$) were refined. The $U_{\rm iso}$ values

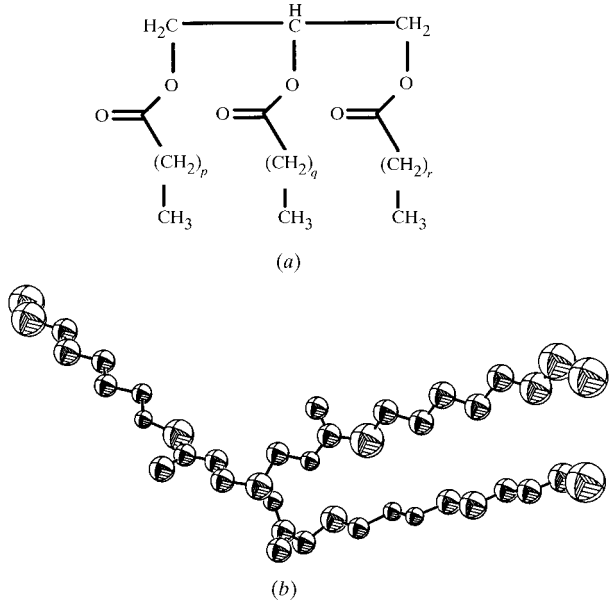

Figure 2
(*a*) Chemical structural diagram of CLC ($p = r = 8$ and $q = 10$), LML ($p = r = 10$ and $q = 12$), MPM ($p = r = 12$ and $q = 14$) and PSP ($p = r = 14$ and $q = 16$). (*b*) *PLATON* (Spek, 2000) representation of the crystal structure of β'-CLC.

of all C atoms were coupled as well as the U_{iso} values for all O atoms; the U_{iso} values for H atoms were fixed at 0.05 Å^2. The preferred orientation was refined using the nine coefficients of the symmetrized harmonics-expansion method (Ahtee *et al.*, 1989; Järvinen, 1993).

The crystal structure of β'-MPM has been compared with the structure of β'-CLC in order to determine their structural correspondence. Therefore, matching was performed by minimizing the distance between corresponding C and O atoms, resulting in an overall r.m.s. (root mean square) value expressing the quality of the fit.

2.4. Comparison of β' structures with models

The crystal structure of β'-CLC has been compared with the packing model by Van Langevelde, Van Malssen, Sonneveld *et al.* (1999) and with the recently published atomic model by Van de Streek *et al.* (1999). The atomic coordinates of the latter were obtained from Jacco Van de Streek (CAOS/CAMM Center, Nijmegen, The Netherlands). A comparison was also made between crystal structures of β and β' polymorphs. For the β polymorph the atomic coordinates of the crystal structure of β-PPP were used (Van Langevelde, Van Malssen, Hollander *et al.*, 1999).

For visualization and structural comparison of the structures version 3.0a of the program *PLUVA* (Driessen *et al.*, 1988) was used. Drawings of molecular structures were made using the program *PLATON* (Spek, 2000).

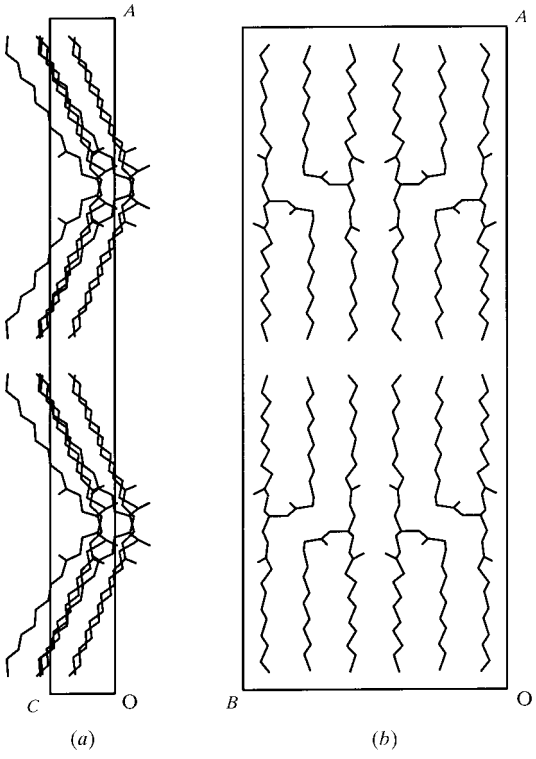

Figure 3
(*a*) Packing diagram of β'-CLC viewed perpendicular to the *ac* plane showing the bending of the molecules. (*b*) Packing diagram of β'-CLC viewed perpendicular to the *ab* plane showing the chain packing.

Table 1
Fractional atomic coordinates and isotropic displacement parameters (Å^2).

Cell parameters of β'-CLC: a = 57.368 (6), b = 22.783 (2), c = 5.6945 (6) Å. The volume is 7443 (1) Å^3 and the space group is *Iba*2, with Z = 8 resulting in a density of 1.04 Mg m^{-3}.

	x	y	z	U_{iso}
C1	0.2394 (4)	0.07597 (7)	0.2021 (13)	0.095 (15)
C2	0.2627 (4)	0.1016 (11)	0.267 (4)	0.119 (17)
C3	0.2699 (3)	0.08108 (6)	0.510 (3)	0.085 (13)
O1*a*	0.2234 (3)	0.0947 (10)	0.366 (4)	0.087 (9)
C1*a*	0.2009 (3)	0.0825 (14)	0.335 (4)	0.082 (13)
O2*a*	0.1942 (4)	0.0588 (11)	0.151 (5)	0.106 (10)
O1*b*	0.2616 (3)	0.1676 (8)	0.292 (4)	0.062 (7)
C1*b*	0.2732 (6)	0.1983 (10)	0.128 (5)	0.092 (15)
O2*b*	0.2814 (4)	0.1784 (10)	−0.050 (5)	0.102 (10)
O1*c*	0.2930 (3)	0.0962 (8)	0.539 (3)	0.061 (7)
C1*c*	0.3031 (4)	0.0770 (13)	0.730 (5)	0.094 (14)
O2*c*	0.2935 (4)	0.0387 (10)	0.850 (4)	0.087 (9)
C2*a*	0.1829 (5)	0.10913 (17)	0.517 (2)	0.16 (2)
C3*a*	0.1610 (4)	0.0697 (2)	0.505 (2)	0.056 (10)
C4*a*	0.1469 (4)	0.08649 (4)	0.7190 (18)	0.070 (12)
C5*a*	0.1211 (4)	0.07030 (6)	0.6884 (18)	0.085 (14)
C6*a*	0.1062 (4)	0.09006 (4)	0.8946 (19)	0.090 (14)
C7*a*	0.0811 (4)	0.06940 (6)	0.8651 (19)	0.116 (17)
C8*a*	0.0662 (4)	0.09357 (5)	1.057 (2)	0.104 (15)
C9*a*	0.0416 (5)	0.06708 (10)	1.039 (2)	0.20 (3)
C10*a*	0.02665 (2)	0.09869 (5)	1.2077 (2)	0.21 (3)
C2*b*	0.27672 (18)	0.2629 (8)	0.188 (3)	0.089 (14)
C3*b*	0.2895 (5)	0.26955 (12)	0.429 (2)	0.118 (17)
C4*b*	0.3149 (4)	0.25383 (4)	0.3795 (17)	0.079 (13)
C5*b*	0.3304 (4)	0.27059 (8)	0.5930 (17)	0.058 (11)
C6*b*	0.3542 (4)	0.24838 (4)	0.5609 (16)	0.056 (11)
C7*b*	0.3696 (4)	0.26984 (4)	0.767 (2)	0.104 (15)
C8*b*	0.3944 (4)	0.24753 (4)	0.749 (2)	0.129 (18)
C9*b*	0.4089 (4)	0.26926 (7)	0.956 (2)	0.095 (15)
C10*b*	0.4327 (4)	0.24288 (5)	0.948 (2)	0.102 (16)
C11*b*	0.4472 (5)	0.26806 (4)	1.150 (2)	0.14 (2)
C12*b*	0.47106 (3)	0.24508 (4)	1.11927 (15)	0.27 (4)
C2*c*	0.3251 (4)	0.11090 (9)	0.817 (3)	0.19 (3)
C3*c*	0.3391 (4)	0.07022 (11)	0.996 (2)	0.102 (15)
C4*c*	0.3622 (4)	0.10017 (5)	1.032 (3)	0.102 (14)
C5*c*	0.3754 (4)	0.07134 (6)	1.226 (2)	0.119 (17)
C6*c*	0.3998 (4)	0.09744 (4)	1.245 (2)	0.115 (16)
C7*c*	0.4133 (4)	0.07067 (11)	1.457 (3)	0.121 (18)
C8*c*	0.4352 (5)	0.10473 (5)	1.498 (3)	0.17 (2)
C9*c*	0.4498 (5)	0.07185 (15)	1.682 (2)	0.23 (3)
C10*c*	0.47335 (3)	0.09280 (4)	1.65463 (15)	0.26 (4)

3. Results and discussion

3.1. Structure of β'-CLC from single-crystal data

The chemical structure diagram and a *PLATON* (Spek, 2000) representation of the crystal structure of β'-CLC are shown in Fig. 2. The fractional atomic coordinates and isotropic atomic displacement parameters (ADPs) are listed in Table 1.[1] Under the experimental conditions given in §2.1 β'-CLC crystallizes in space group *Iba*2 in a chair conformation, characterized by two neighbouring acyl chains (II) and (III) pointing in one direction. The other (I) makes an angle of ∼130° with chains (II) and (III). Bond lengths and angles are listed in Table 2. The molecules are bent at the glycerol moiety

[1] Supplementary data for this paper are available from the IUCr electronic archives (Reference: NA0109). Services for accessing these data are described at the back of the journal.

and packed with the chains along each other, as imposed by the *Iba*2 symmetry resulting in a layered structure (Fig. 3). Layers of chains are succeeded by either planes of methyl end-groups or by planes of glycerol moieties. The layers are parallel to the *bc* plane. The direction of the 65° tilt of the chains with respect to the methyl end-group plane is changing per chain layer. The zigzag planes of the acyl chains are orthogonally packed, as is typical for a β' polymorph (Abrahamsson *et al.*, 1978).

Since the molecular structure fits the $2mF_o - DF_{calc}$ electron-density map very well, it can be concluded that this crystal structure indeed expresses the measured intensity values (Fig. 4). Although a rather high R value remains after refinement, no significant maxima were observed in the ΔF synthesis. Furthermore, refinement in monoclinic space group $I2$ with two molecules in the asymmetric unit did not lead to more accurate results. The isotropic ADP values of β'-CLC are somewhat larger than ADPs for comparable structures, such as β-PPP (Van Langevelde, Van Malssen, Hollander *et al.*, 1999). Especially at the end of the acyl chains the isotropic APDs are large, denoting a larger mobility of the chain ends.

3.2. Structure of other series members from powder data

The unit-cell parameters of β'-MPM measured at room temperature were refined to a = 76.21 (4), b = 22.63 (1) and c = 5.673 (2) Å resulting in a cell volume of 9784 (8) Å^3. As for β'-CLC, the space group for β'-MPM is *Iba*2. With eight $C_{47}H_{90}O_6$ molecules in the unit cell the calculated density is 1.020 Mg m^{-3}. The FPD applied to 1.5–24.0° 2θ of the synchrotron pattern resulted in an R_p of 0.079, an wR_p of 0.114 and a χ^2 of 4.86. Rietveld refinement applied to a 2θ range from 2.0 to 27.0° resulted in a final fit between the calculated and experimental powder pattern with an R_p value of 0.057, an wR_p of 0.074 an R_{Bragg} of 0.126 and a χ^2 of 2.92 (Fig. 5). Without correction for preferred orientation the R_p value was 0.073, wR_p = 0.102, R_{Bragg} = 0.155 and χ^2 = was 4.1. The refined preferred orientation parameters are listed in Table 3. The refined crystal structure of β'-MPM is shown in Fig. 6. Fractional atomic coordinates and geometric parameters are listed in Tables 4 and 5, respectively. β'-MPM is crystallized in a chair conformation and the zigzag planes of the acyl chains are orthogonally packed. The structure of β'-MPM is almost identical to the structure of β'-CLC, as expressed by an overall r.m.s. value of 0.095.

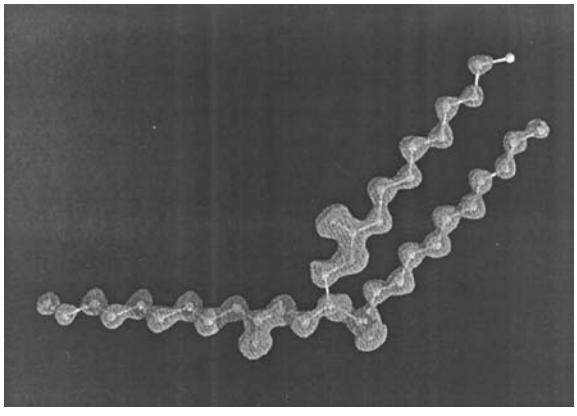

Figure 4
$2mF_o - DF_{calc}$ electron-density map of β'-CLC contoured at the 2σ level superposed with the final structural model.

Table 2
Selected geometric parameters (Å, °) for β'-CLC.

C1—O1*a*	1.38 (3)	C4*b*—C5*b*	1.55 (2)
C1—C2	1.50 (3)	C5*b*—C6*b*	1.47 (3)
C2—O1*b*	1.51 (3)	C6*b*—C7*b*	1.55 (2)
C3—O1*c*	1.38 (3)	C7*b*—C8*b*	1.51 (3)
O1*a*—C1*a*	1.33 (3)	C8*b*—C9*b*	1.53 (2)
C1*a*—O2*a*	1.24 (4)	C9*b*—C10*b*	1.49 (3)
C1*a*—C2*a*	1.59 (3)	C10*b*—C11*b*	1.53 (2)
C2*a*—C3*a*	1.55 (3)	C11*b*—C12*b*	1.48 (3)
C3*a*—C4*a*	1.51 (2)	O1*c*—C1*c*	1.31 (3)
C4*a*—C5*a*	1.53 (3)	C1*c*—O2*c*	1.24 (4)
C5*a*—C6*a*	1.52 (2)	C1*c*—C2*c*	1.56 (3)
C6*a*—C7*a*	1.52 (3)	C2*c*—C3*c*	1.59 (2)
C7*a*—C8*a*	1.49 (2)	C3*c*—C4*c*	1.51 (3)
C8*a*—C9*a*	1.54 (4)	C4*c*—C5*c*	1.49 (2)
C9*a*—C10*a*	1.48 (2)	C5*c*—C6*c*	1.52 (3)
O1*b*—C1*b*	1.34 (3)	C6*c*—C7*c*	1.56 (2)
C1*b*—O2*b*	1.20 (4)	C7*c*—C8*c*	1.50 (3)
C1*b*—C2*b*	1.53 (3)	C8*c*—C9*c*	1.54 (3)
C2*b*—C3*b*	1.56 (2)	C9*c*—C10*c*	1.44 (3)
C3*b*—C4*b*	1.53 (3)		
O1*a*—C1—C2	107.8 (13)	C4*b*—C3*b*—C2*b*	105.4 (11)
O1*b*—C2—C1	112.0 (16)	C3*b*—C4*b*—C5*b*	110.3 (11)
O1*b*—C2—C3	103.5 (15)	C6*b*—C5*b*—C4*b*	110.5 (10)
C1—C2—C3	110.3 (15)	C5*b*—C6*b*—C7*b*	109.2 (10)
O1*c*—C3—C2	107.1 (15)	C8*b*—C7*b*—C6*b*	112.4 (11)
C1*a*—O1*a*—C1	119 (2)	C7*b*—C8*b*—C9*b*	110.6 (11)
O2*a*—C1*a*—O1*a*	120 (2)	C10*b*—C9*b*—C8*b*	110.0 (11)
O2*a*—C1*a*—C2*a*	121.4 (18)	C9*b*—C10*b*—C11*b*	108.8 (11)
O1*a*—C1*a*—C2*a*	118 (2)	C12*b*—C11*b*—C10*b*	106.3 (10)
C3*a*—C2*a*—C1*a*	106.0 (11)	C1*c*—O1*c*—C3	116.3 (18)
C4*a*—C3*a*—C2*a*	104.5 (10)	O2*c*—C1*c*—O1*c*	120 (2)
C3*a*—C4*a*—C5*a*	111.3 (11)	O2*c*—C1*c*—C2*c*	122 (2)
C6*a*—C5*a*—C4*a*	112.4 (11)	O1*c*—C1*c*—C2*c*	117 (2)
C5*a*—C6*a*—C7*a*	110.7 (11)	C1*c*—C2*c*—C3*c*	108.9 (13)
C8*a*—C7*a*—C6*a*	110.4 (11)	C4*c*—C3*c*—C2*c*	105.5 (10)
C7*a*—C8*a*—C9*a*	109.5 (11)	C5*c*—C4*c*—C3*c*	110.5 (11)
C10*a*—C9*a*—C8*a*	107.3 (8)	C4*c*—C5*c*—C6*c*	110.5 (11)
C1*b*—O1*b*—C2	115.7 (19)	C5*c*—C6*c*—C7*c*	111.2 (11)
O2*b*—C1*b*—O1*b*	126 (2)	C8*c*—C7*c*—C6*c*	109.6 (11)
O2*b*—C1*b*—C2*b*	120 (2)	C7*c*—C8*c*—C9*c*	108.2 (11)
O1*b*—C1*b*—C2*b*	114 (2)	C10*c*—C9*c*—C8*c*	105.9 (11)
C1*b*—C2*b*—C3*b*	110.8 (15)		

The unit-cell parameters of β'-LML, β'-MPM and β'-PSP, as refined from the high-resolution XRPD data [λ = 0.445348 (1) Å] obtained at T = 250 K, show that LML and MPM at this temperature are crystallized in a monoclinic lattice and PSP in an orthorhombic lattice (Table 6). Since the b axis has been chosen as unique, the orthorhombic unit cells (CLC from single-crystal data, MPM from powder data at room temperature and PSP from powder data at T = 250 K) were transformed. For β'-LML the symmetry-related reflections (hkl and $hk\bar{l}$) are significantly split, resulting in a β of 90.4°, whereas for β'-MPM these reflections are just broadened resulting in a β of 90.2°. For β'-PSP broadening of these reflections is hardly noticeable and β refined to 90.00 (2)°. The XRPD patterns of all these TAGs show identical extinction conditions corresponding to the orthorhombic space group

Table 3
Refined preferred orientation coefficients of β'-MPM.

ijp	*Cijp*
20+	−0.054
22+	0.125
40+	−0.405
42+	−0.552
44+	−0.142
60+	0.593
62+	−0.060
64+	−0.285
66+	−0.041

*Ic*2*a* (or *Icma*). However, this space group is impossible for a monoclinic lattice and therefore the correct space group for the monoclinic ones is *I*2. In contrast to earlier work (Van Langevelde, Van Malssen, Sonneveld *et al.*, 1999), a linear increase of the *c* axis and unit-cell volume with increasing acyl-chain length is observed (Table 6 and Fig. 7).

It is remarkable that β'-MPM measured at room temperature was undoubtedly crystallized in an orthorhombic lattice, whereas the β parameter of β'-MPM measured at T = 250 K significantly deviates from 90.0°. Furthermore, deviation from orthorhombic symmetry is decreasing with increasing acyl-chain length (Table 6). Therefore, we conclude that the crystal structure of β'-PSP at T = 250 K is an isomorphic homologue of β'-CLC and orthorhombic β'-MPM. Therefore, β'-PSP may

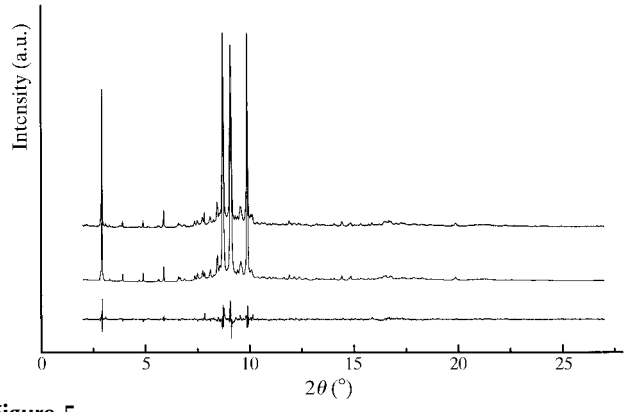

Figure 5
Synchrotron powder-diffraction pattern [λ = 0.650515 (1) Å] of orthorhombic β'-MPM (upper); the pattern as calculated from the refined crystal structure (middle) and the difference between these patterns (lower).

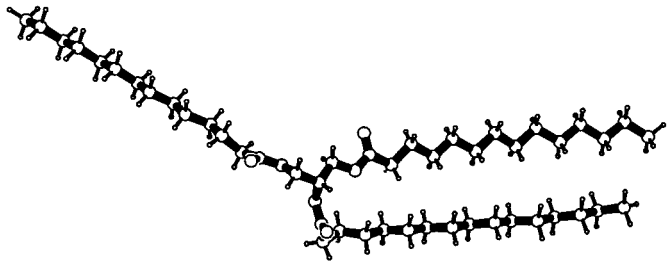

Figure 6
PLATON (Spek, 2000) representation of the crystal structure of β'-MPM.

Table 4
Fractional atomic coordinates of β'-MPM after Rietveld refinement.

Cell parameters of β'-MPM: a = 76.21 (4), b = 22.63 (1), c = 5.673 (2) Å. The volume is 9784 (8) Å^3 and the space group is *Iba*2, with Z = 8 resulting in a density of 1.02 Mg m^{-3}.

	x	*y*	*z*	U_{iso}
C1	0.242 (2)	0.074 (6)	−0.839 (10)	0.018
C2	0.259 (2)	0.100 (6)	−0.77 (2)	0.018
C3	0.264 (2)	0.081 (6)	−0.528 (17)	0.018
O1*a*	0.229 (2)	0.094 (4)	−0.681 (13)	0.018
C1*a*	0.213 (2)	0.081 (6)	−0.713 (19)	0.018
O2*a*	0.208 (2)	0.055 (4)	−0.896 (12)	0.018
C2*a*	0.199 (3)	0.111 (6)	−0.550 (16)	0.018
C3*a*	0.182 (3)	0.071 (6)	−0.558 (17)	0.018
C4*a*	0.172 (2)	0.090 (7)	−0.35 (2)	0.018
C5*a*	0.153 (3)	0.073 (7)	−0.37 (2)	0.018
C6*a*	0.142 (2)	0.094 (7)	−0.16 (2)	0.018
C7*a*	0.123 (3)	0.071 (5)	−0.17 (3)	0.018
C8*a*	0.113 (2)	0.095 (6)	0.025 (17)	0.018
C9*a*	0.095 (2)	0.066 (7)	0.023 (18)	0.018
C10*a*	0.083 (2)	0.096 (7)	0.21 (2)	0.018
C11*a*	0.065 (2)	0.067 (7)	0.20 (2)	0.018
C12*a*	0.053 (3)	0.096 (7)	0.381 (18)	0.018
C13*a*	0.035 (3)	0.067 (7)	0.373 (18)	0.018
C14*a*	0.023 (2)	0.097 (7)	0.555 (19)	0.018
O1*b*	0.258 (2)	0.167 (4)	−0.757 (14)	0.018
C1*b*	0.267 (3)	0.197 (6)	−0.92 (2)	0.018
O2*b*	0.273 (2)	0.178 (4)	−1.103 (13)	0.018
C2*b*	0.270 (2)	0.262 (6)	−0.87 (3)	0.018
C3*b*	0.280 (3)	0.269 (6)	−0.63 (2)	0.018
C4*b*	0.298 (3)	0.251 (6)	−0.68 (2)	0.018
C5*b*	0.310 (2)	0.268 (6)	−0.47 (2)	0.018
C6*b*	0.328 (2)	0.245 (7)	−0.50 (2)	0.018
C7*b*	0.339 (2)	0.267 (7)	−0.29 (2)	0.018
C8*b*	0.358 (2)	0.244 (7)	−0.31 (3)	0.018
C9*b*	0.368 (3)	0.267 (6)	−0.10 (2)	0.018
C10*b*	0.386 (3)	0.241 (6)	−0.109 (19)	0.018
C11*b*	0.397 (2)	0.267 (7)	0.09 (2)	0.018
C12*b*	0.416 (2)	0.244 (8)	0.08 (2)	0.018
C13*b*	0.426 (3)	0.267 (6)	0.29 (2)	0.018
C14*b*	0.444 (2)	0.239 (6)	0.29 (2)	0.018
C15*b*	0.455 (2)	0.261 (7)	0.505 (19)	0.018
C16*b*	0.473 (2)	0.231 (7)	0.51 (2)	0.018
O1*c*	0.281 (2)	0.095 (4)	−0.498 (10)	0.018
C1*c*	0.289 (2)	0.077 (7)	−0.303 (18)	0.018
O2*c*	0.281 (2)	0.041 (4)	−0.174 (13)	0.018
C2*c*	0.305 (2)	0.110 (7)	−0.22 (2)	0.018
C3*c*	0.316 (2)	0.070 (6)	−0.039 (18)	0.018
C4*c*	0.333 (3)	0.099 (6)	−0.009 (16)	0.018
C5*c*	0.343 (2)	0.071 (6)	0.19 (2)	0.018
C6*c*	0.361 (2)	0.096 (7)	0.20 (2)	0.018
C7*c*	0.372 (3)	0.070 (6)	0.41 (2)	0.018
C8*c*	0.388 (2)	0.104 (7)	0.443 (15)	0.018
C9*c*	0.399 (2)	0.072 (7)	0.629 (19)	0.018
C10*c*	0.418 (2)	0.095 (7)	0.615 (19)	0.018
C11*c*	0.429 (2)	0.068 (6)	0.81 (2)	0.018
C12*c*	0.448 (3)	0.090 (6)	0.79 (2)	0.018
C13*c*	0.459 (3)	0.064 (6)	0.987 (17)	0.018
C14*c*	0.478 (2)	0.088 (6)	0.96 (2)	0.018

be obtained by extrapolation from β'-MPM, as described for the β-C$_n$C$_n$C$_n$-type (n = even) TAGs series (Van Langevelde, Van Malssen, Hollander *et al.*, 1999). Since monoclinic β'-LML and β'-MPM differ from the series by a small deviation in the β parameter only, their structures also seem to be similar to β'-CLC and orthorhombic β'-MPM. Possibly, the chain-end mobility, as observed at the crystal structure of β'-CLC, is less for the lower-temperature measurements and the positions of

Table 5
Selected geometric parameters (Å^2, °) for β'-MPM.

C1—O1*a*	1.41 (17)	C5*b*—C6*b*	1.5 (2)
C1—C2	1.5 (2)	C6*b*—C7*b*	1.5 (2)
C2—C3	1.50 (17)	C7*b*—C8*b*	1.5 (2)
C2—O1*b*	1.52 (16)	C8*b*—C9*b*	1.5 (2)
C3—O1*c*	1.3 (2)	C9*b*—C10*b*	1.5 (3)
O1*a*—C1*a*	1.3 (2)	C10*b*—C11*b*	1.5 (2)
C1*a*—O2*a*	1.25 (15)	C11*b*—C12*b*	1.5 (2)
C1*a*—C2*a*	1.6 (2)	C12*b*—C13*b*	1.5 (2)
C2*a*—C3*a*	1.6 (3)	C13*b*—C14*b*	1.5 (3)
C3*a*—C4*a*	1.5 (2)	C14*b*—C15*b*	1.56 (19)
C4*a*—C5*a*	1.5 (3)	C15*b*—C16*b*	1.5 (2)
C5*a*—C6*a*	1.5 (2)	O1*c*—C1*c*	1.33 (15)
C6*a*—C7*a*	1.5 (3)	C1*c*—O2*c*	1.25 (17)
C7*a*—C8*a*	1.5 (2)	C1*c*—C2*c*	1.5 (2)
C8*a*—C9*a*	1.5 (2)	C2*c*—C3*c*	1.6 (2)
C9*a*—C10*a*	1.5 (2)	C3*c*—C4*c*	1.5 (3)
C10*a*—C11*a*	1.5 (2)	C4*c*—C5*c*	1.5 (2)
C11*a*—C12*a*	1.5 (2)	C5*c*—C6*c*	1.5 (2)
C12*a*—C13*a*	1.5 (3)	C6*c*—C7*c*	1.6 (2)
C13*a*—C14*a*	1.5 (2)	C7*c*—C8*c*	1.5 (3)
O1*b*—C1*b*	1.35 (19)	C8*c*—C9*c*	1.53 (18)
C1*b*—O2*b*	1.20 (17)	C9*c*—C10*c*	1.5 (2)
C1*b*—C2*b*	1.5 (2)	C10*c*—C11*c*	1.53 (19)
C2*b*—C3*b*	1.6 (2)	C11*c*—C12*c*	1.5 (3)
C3*b*—C4*b*	1.5 (3)	C12*c*—C13*c*	1.5 (2)
C4*b*—C5*b*	1.6 (2)	C13*c*—C14*c*	1.6 (3)
O1*a*—C1—C2	109	C6*b*—C5*b*—C4*b*	112 (12)
C1—C2—O1*b*	112 (12)	C5*b*—C6*b*—C7*b*	109 (11)
C3—C2—O1*b*	104 (10)	C6*b*—C7*b*—C8*b*	112 (12)
C1—C2—C3	110 (11)	C9*b*—C8*b*—C7*b*	109 (13)
O1*c*—C3—C2	107 (10)	C8*b*—C9*b*—C10*b*	108 (12)
C1*a*—O1*a*—C1	121	C9*b*—C10*b*—C11*b*	109 (11)
O2*a*—C1*a*—O1*a*	121 (13)	C12*b*—C11*b*—C10*b*	110 (13)
O2*a*—C1*a*—C2*a*	119 (14)	C13*b*—C12*b*—C11*b*	108 (13)
O1*a*—C1*a*—C2*a*	118 (12)	C14*b*—C13*b*—C12*b*	108 (12)
C1*a*—C2*a*—C3*a*	107 (11)	C13*b*—C14*b*—C15*b*	110 (11)
C4*a*—C3*a*—C2*a*	103 (11)	C16*b*—C15*b*—C14*b*	110 (11)
C3*a*—C4*a*—C5*a*	112 (13)	C1*c*—O1*c*—C3	118 (11)
C4*a*—C5*a*—C6*a*	113 (12)	O2*c*—C1*c*—O1*c*	118 (14)
C5*a*—C6*a*—C7*a*	111 (13)	O2*c*—C1*c*—C2*c*	123 (11)
C8*a*—C7*a*—C6*a*	108 (12)	O1*c*—C1*c*—C2*c*	118 (13)
C7*a*—C8*a*—C9*a*	108 (12)	C1*c*—C2*c*—C3*c*	110 (12)
C8*a*—C9*a*—C10*a*	110 (11)	C4*c*—C3*c*—C2*c*	106 (11)
C11*a*—C10*a*—C9*a*	109 (12)	C3*c*—C4*c*—C5*c*	111 (11)
C12*a*—C11*a*—C10*a*	110 (13)	C4*c*—C5*c*—C6*c*	111 (13)
C11*a*—C12*a*—C13*a*	110 (12)	C5*c*—C6*c*—C7*c*	113 (13)
C12*a*—C13*a*—C14*a*	109 (12)	C8*c*—C7*c*—C6*c*	110 (11)
C1*b*—O1*b*—C2	116 (11)	C7*c*—C8*c*—C9*c*	107 (12)
O2*b*—C1*b*—O1*b*	127 (13)	C8*c*—C9*c*—C10*c*	109 (11)
O2*b*—C1*b*—C2*b*	117 (14)	C11*c*—C10*c*—C9*c*	110 (11)
O1*b*—C1*b*—C2*b*	115 (11)	C10*c*—C11*c*—C12*c*	109 (11)
C1*b*—C2*b*—C3*b*	110 (11)	C13*c*—C12*c*—C11*c*	109 (13)
C4*b*—C3*b*—C2*b*	106 (11)	C12*c*—C13*c*—C14*c*	108 (12)
C3*b*—C4*b*—C5*b*	110 (11)		

the chain-end atoms deviate slightly from their corresponding atomic positions in orthorhombic symmetry. This small deviation may force the symmetry to be monoclinic. Since this deviation becomes smaller with increasing chain length, it is assumed that the orthogonal–lateral chain packing of the TAG molecules is more stable at longer chain lengths, preventing considerable chain-end mobility.

The characteristic powder diffraction pattern of β'-TAGs originates from the orthogonal lateral chain packing denoted by $O_\perp$ (Abrahamsson *et al.*, 1978). Since many scatterers are at the lattice planes which are (nearly) parallel to the acyl chains,

Table 6
Refined cell parameters of β'-$C_nC_{n+2}C_n$-type TAGs.

In order to compare these cell parameters more easily, the unit cells have been transformed to an unique *b* axis. β'-CLC results were determined from single-crystal data and for the other compounds from high-resolution powder data.

	β'-CLC	β'-LML	β'-MPM	β'-MPM	β'-PSP
a (Å)	22.783 (2)	22.650 (2)	22.63 (1)	22.660 (2)	22.829 (4)
b (Å)	5.6945 (6)	5.6513 (4)	5.673 (2)	5.6261 (7)	5.5946 (8)
c (Å)	57.368 (6)	67.183 (6)	76.21 (4)	76.217 (8)	85.48 (2)
α (°)	90.0	90.0	90.0	90.0	90.0
β (°)	90.0	90.391 (7)	90.0	90.18 (1)	90.00 (2)
γ (°)	90.0	90.0	90.0	90.0	90.0
V (Å^3)	7443 (1)	8599.3 (9)	9784 (8)	9717 (1)	10917 (3)
Space group	*Ic2a*	*I*2	*Ic2a*	*I*2	*Ic2a*
Chemical formula	$C_{35}H_{66}O_6$	$C_{41}H_{78}O_6$	$C_{47}H_{90}O_6$	$C_{47}H_{90}O_6$	$C_{53}H_{102}O_6$
Z	8	8	8	8	8
D_{calc} (Mg m^{-3})	1.04	1.03	1.02	1.03	1.02
T (K)	295	250	295	250	250

this results in strong reflections in the X-ray powder diagram (Fig. 8 and Table 7). The lattice plane distances for the lattice planes (nearly) parallel to the acyl chains show that reflections with identical indices of different series members do not have exactly the same *d*-spacing values (Table 7). As a result, the characteristic region of the XRPD pattern and the lateral chain packing is slightly different for each series member of this β'-stable TAG series.

3.3. (Dis)similarities between β' structures and models

The unit-cell parameters and space group of β'-CLC and β'-MPM correspond well to those determined from Guinier data previously (Van Langevelde, Van Malssen, Sonneveld *et al.*, 1999). However, in contrast to their β'-CLC packing model, having intramolecular parallel acyl-chain zigzag planes, β'-CLC adopts an $O_\perp$ lateral chain packing with intramolecular orthogonal zigzag planes. Since at that moment straight asymmetric tuning-fork conformations were only available, this type of TAG molecule was used for their packing model. As a result, no tilt of the acyl chains with respect to the methyl end-group plane has been found. In retrospect, the assumption that the β'-$C_nC_{n+2}C_n$-type (*n* = even) TAG molecules are

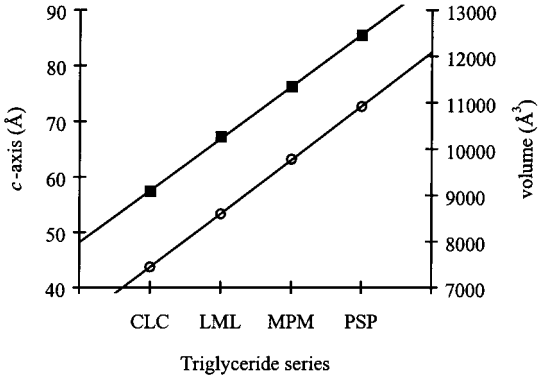

Figure 7
The length of the *c* axis (black squares) and the unit-cell volume (open circles) of β'-CLC, β'-LML, β'-MPM and β'-PSP (Table 6).

Table 7
Characteristic d spacings (Å) for β'-$C_nC_{n+2}C_n$-type (n = even) TAG series.

	$d(314)$	$d(31\bar{4})$	$d(316)$	$d(31\bar{6})$	$d(318)$	$d(31\bar{8})$	$d(600)$
β'-CLC†	4.342	4.342	4.113	4.113	3.845	3.845	3.797
β'-LML‡	4.373	4.364	4.201	4.189	3.990	3.976	3.775
β'-MPM†	4.411	4.411	4.270	4.270	4.094	4.094	3.772
β'-MPM‡	4.392	4.389	4.254	4.249	4.081	4.075	3.777
β'-PSP†	4.410	4.410	4.298	4.298	4.153	4.153	3.805

† Orthorhombic lattice. ‡ Monoclinic lattice. See Table 6 for unit-cell parameters.

in a straight asymmetric tuning-fork conformation was incorrect, although it was already recognized that with TAG molecules in a chair conformation the relative phase stability of the β' polymorph can be explained.

The crystal structure model by Van de Streek *et al.* (1999) accommodates most of the characteristic elements of the β'-CLC crystal structure. Their TAG molecules are bent at the glycerol moiety, adopt an $O_\perp$ lateral chain packing with intramolecular orthogonal zigzag planes and are in a chair conformation. Consequently, their calculated X-ray powder diffractogram is in good agreement with the experimental one. However, some deviations between their model and the experimental crystal structure can be observed. The conformation of their glycerol moiety is not completely correct, which results in a significant difference (~4 Å) between the c axis of their model and the experimental one. Furthermore, the orientations of the acyl-chain zigzag planes with respect to the axes through the chains differ by 90° with the experimental ones. Since this orientation differs by 90° for all three acyl chains, the overall $O_\perp$ chain packing of their model is still the same as the chain packing in the experimental crystal structure, but the carbonyl moiety of the second chain just points in the opposite direction.

The crystal structures of the known β and β' polymorphs differ in three major aspects:

(i) the molecules of the β polymorph are straight, whereas the molecules of the β' polymorph are bent at the glycerol moiety,

(ii) the β polymorph has intramolecular parallel zigzag planes, whereas the β' polymorph has intramolecular orthogonal zigzag planes, and

(iii) the β polymorph is crystallized in an asymmetric tuning-fork conformation, whereas the β' polymorph adopts a chair conformation.

All these differences affect the conformation of the glycerol moiety (Fig. 9). The typical conformation of the glycerol moiety in the β polymorph is a consequence of a straight structure having intramolecular parallel zigzag planes and an asymmetric tuning-fork conformation. Similarly, the typical conformation of the glycerol moiety in the β' polymorph is a consequence of a bent structure having intramolecular orthogonal zigzag planes and a chair conformation. Since the relative stability of the polymorphic phases is determined by differences in chain length and saturation (De Jong, 1980), the crystallizing polymorph is not determined by the typical glycerol moiety of the β and β' polymorphs.

From the crystal structures of these β' and β polymorphs the relative stability of the β' polymorph for the $C_nC_{n+2}C_n$-type (n = even) TAG series can be explained. Since the crystal structure of these series members are in a chair conformation a solid-state transformation to a β polymorph, typically crystallized in a tuning-fork conformation, is impossible. Therefore, it is expected that the crystal structure of a β' polymorph of β-stable TAGs will differ from the structures reported here.

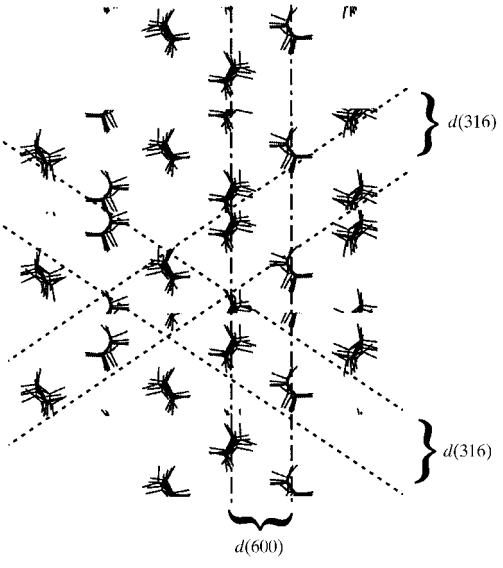

Figure 8
Crystal structure of β'-CLC (transformed to a unique b axis) with the acyl chains perpendicular to the plane of the paper. The lattice planes responsible for the characteristic d spacings are indicated (Tables 6 and 7).

The investigations were supported by The Netherlands Foundation for Chemical Research (NWO/CW) with financial aid from The Netherlands Technology Foundation (STW).

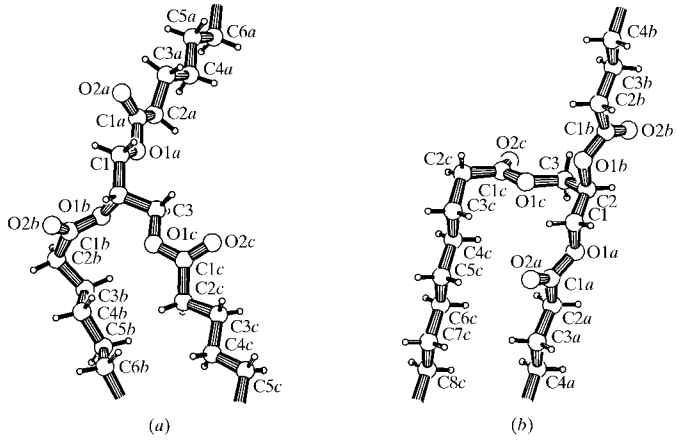

Figure 9
PLATON (Spek, 2000) representation of the glycerol moiety of the crystal structure of (*a*) β'-CLC and (*b*) β-PPP (Van Langevelde, Van Malssen, Hollander *et al.*, 1999).

The authors thank Unilever Research Laboratory (Vlaardingen, The Netherlands) for providing CLC crystals. The authors also thank the ESRF (Grenoble, France) for the opportunity to perform the synchrotron experiments, and Professor Dr Å. Kvick and Dr A. N. Fitch for their invaluable help at ID11 (single-crystal diffraction measurements) and BM16 (high-resolution powder diffraction measurements), respectively. Bruker AXS is kindly thanked for making available their single-crystal software packages. Jacco Van de Streek is thanked for providing the coordinates of his β'-CLC structure model.

References

Abrahamsson, S., Dahlén, B., Löfgren, H. & Pascher, I. (1978). *Prog. Chem. Fats Other Lipids*, **16**, 125–143.
Ahtee, M., Nurmela, M., Suortti, P. & Järvinen, M. (1989). *J. Appl. Cryst.* **22**, 261–268.
Arishima, T. & Sato, K. (1989). *J. Am. Oil Chem. Soc.* **66**, 1614–1617.
Birker, P. J. M. W. L., De Jong, S., Roijers, E. C. & Van Soest, T. C. (1991). *J. Am. Oil Chem. Soc.* **68**, 895–906.
Boistelle, R., Simon, B. & Pèpe, G. (1976). *Acta Cryst.* B**32**, 1240–1243.
Bruker AXS Inc. (1996). *SAINT*. Version 4.0. Bruker AXS Inc., Madison, Wisconsin, USA.
Bruker AXS Inc. (1998). *SMART*. Version 5.0. Bruker AXS Inc., Madison, Wisconsin, USA.
Chernyshev, V. V. & Schenk, H. (1998). *Z. Kristallogr.* **213**, 1–3.
De Jong, S. (1980). PhD thesis. University of Utrecht, The Netherlands.
De Jong, S. & Van Soest, T. C. (1978). *Acta Cryst.* B**34**, 1570–1583.
Doyne, T. H. & Gordon, J. T. (1968). *J. Am. Oil Chem. Soc.* **45**, 333–334.
Driessen, R. A. J., Loopstra, B. O., De Bruijn, D. P., Kuipers, H. P. C. E. & Schenk, H. (1988). *J. Comput.-Aided Mol. Des.* **2**, 225–233.
Fitch, A. N. (1996). *Materials Science Forum*, Vol. 228, edited by R. J. Cernik, R. Delhez and E. J. Mittemeijer, pp. 219–222. Aedermannsdorf: Trans Tech Publications.
Gibon, V., Blanpain, P., Norberg, B. & Durant, F. (1984). *Bull. Soc. Chim. Belg.* **93**, 27–34.
Goto, M., Kodali, D. R., Small, D. M., Honda, K., Kozawa, K. & Uchida, T. (1992). *Proc. Nat. Acad. Sci. USA*, **89**, 8083–8086.
Hagemann, J. W. (1988). *Crystallization and Polymorphism of Fats and Fatty Acids*, edited by N. Garti and K. Sato, pp. 9–96. New York and Basel: Marcel Dekker Inc.
Hall, S. R., King, G. S. D. & Stewart, J. M. (1995). *Xtal.* Version 3.5. Universities of Western Australia, Australia, Geneva, Switzerland, and Maryland, USA.
Hernqvist, L. (1988). *Fat Sci. Technol.* **90**, 451–454.
Hernqvist, L. & Larsson, K. (1982). *Fette Seifen Anstrichm.* **84**, 349–354.
Holland, T. J. B. & Redfern, S. A. T. (1997). *Mineral Mag.* **61**, 65–77.
Järvinen, M. (1993). *J. Appl. Cryst.* **26**, 525–531.
Jensen, L. H. & Mabis, A. J. (1963). *Nature*, **197**, 681–682.
Jensen, L. H. & Mabis, A. J. (1966). *Acta Cryst.* **21**, 770–781.
Jones, T. A., Zou, J. Y., Cowan, S. W. & Kjeldgaard, M. (1991). *Acta Cryst.* A**47**, 110–119.
Kvick, Å. & Wulff, M. (1992). *Rev. Sci. Instrum.* **63**, 1073–1076.
Larsson, K. (1965*a*). *Arkiv Kemi*, **23**, 1–15.
Larsson, K. (1965*b*). *Arkiv Kemi*, **23**, 35–56.
Miller, R., Gallo, S. M., Khalak, H. G. & Weeks, C. M. (1994). *J. Appl. Cryst.* **27**, 613–621.
Molecular Simulations Inc. (1995). *Cerius*2. Release 2.0. Biosym Molecular Simulations Inc., San Diego, USA.
Murshudov, G. N., Vagin, A. A. & Dodson, E. J. (1997). *Acta Cryst.* D**53**, 240–255.
Number 4 Collaborative Computational Project (1994). *Acta Cryst.* D**50**, 760–763.
Sato, K. (1996). *Adv. Appl. Lipid Res.* **2**, 213–268.
Simpson, T. D. & Hagemann, J. W. (1982). *J. Am. Oil Chem. Soc.* **59**, 169–171.
Spek, A. L. (2000). *PLATON*. Utrecht University, Utrecht, The Netherlands.
Toraya, H. (1986). *J. Appl. Cryst.* **19**, 440–447.
Van de Streek, J., Verwer, P., De Gelder, R. & Hollander, F. (1999). *J. Am. Oil Chem. Soc.* **76**, 1333–1341.
Van Langevelde, A., Van Malssen, K., Hollander, F., Peschar, R. & Schenk, H. (1999). *Acta Cryst.* B**55**, 114–122.
Van Langevelde, A., Van Malssen, K., Sonneveld, E., Peschar, R. & Schenk, H. (1999). *J. Am. Oil Chem. Soc.* **76**, 603–609.
Zlokazov, V. B. & Chernyshev, V. V. (1992). *J. Appl. Cryst.* **25**, 447–451.